

Direct high-resolution transmission electron microscopy observation of tetragonal nanotwins within the monoclinic M C phase of $\text{Pb}(\text{Mg}(1/3)\text{Nb}(2/3))\text{O}_3-0.35\text{PbTiO}_3$ crystals

Somnath Bhattacharyya, J. R. Jinschek, Hu Cao, Yu U. Wang, Jiefang Li, and D. Viehland

Citation: [Applied Physics Letters](#) **92**, 142904 (2008); doi: 10.1063/1.2908228

View online: <http://dx.doi.org/10.1063/1.2908228>

View Table of Contents: <http://scitation.aip.org/content/aip/journal/apl/92/14?ver=pdfcov>

Published by the [AIP Publishing](#)

Articles you may be interested in

[Strain and in-plane orientation effects on the ferroelectricity of \(111\)-oriented tetragonal \$\text{Pb}\(\text{Zr}0.35\text{Ti}0.65\)\text{O}_3\$ thin films prepared by metal organic chemical vapor deposition](#)

[Appl. Phys. Lett.](#) **90**, 222901 (2007); 10.1063/1.2743748

[Monoclinic M C vs orthorhombic in \[001 \] and \[110 \] electric-field-cooled \$\text{Pb}\(\text{Mg}\(1/3\)\text{Nb}\(2/3\)\text{O}_3\) - 35\%\$ \$\text{PbTiO}_3\$ Crystals](#)

[Appl. Phys. Lett.](#) **88**, 072915 (2006); 10.1063/1.2175497

[Abnormal phase transitions for tetragonal \$\(1-x\)\text{Pb}\(\text{Mg}\(1/3\)\text{Nb}\(2/3\)\text{O}_3\) - x\text{PbTiO}_3\$ single crystals at low temperature](#)

[J. Appl. Phys.](#) **96**, 6574 (2004); 10.1063/1.1808906

[In-plane dielectric properties of epitaxial \$0.65\text{Pb}\(\text{Mg}\(1/3\)\text{Nb}\(2/3\)\text{O}_3\) - 0.35\text{PbTiO}_3\$ thin films in a very wide frequency range](#)

[Appl. Phys. Lett.](#) **85**, 1580 (2004); 10.1063/1.1784517

[Dielectric and ferroelectric behaviors in \$\text{Pb}\(\text{Mg}\(1/3\)\text{Nb}\(2/3\)\text{O}_3\) - \text{PbTiO}_3\$ rhombohedral tetragonal superlattices](#)

[Appl. Phys. Lett.](#) **85**, 979 (2004); 10.1063/1.1777821



Re-register for Table of Content Alerts

Create a profile.



Sign up today!



Direct high-resolution transmission electron microscopy observation of tetragonal nanotwins within the monoclinic M_C phase of $\text{Pb}(\text{Mg}_{1/3}\text{Nb}_{2/3})\text{O}_3\text{-}0.35\text{PbTiO}_3$ crystals

Somnath Bhattacharyya,^{a)} J. R. Jinschek,^{b)} Hu Cao, Yu U. Wang, Jiefang Li, and D. Viehland

Department of Materials Science and Engineering, Virginia Tech, Blacksburg, Virginia 24061, USA

(Received 5 March 2008; accepted 24 March 2008; published online 9 April 2008)

We report on the direct observation of tetragonal nanodomains within an average monoclinic M_C phase of $\text{Pb}(\text{Mg}_{1/3}\text{Nb}_{2/3})\text{O}_3\text{-}0.35\text{PbTiO}_3$ single crystals by high-resolution transmission electron microscopy. These nanodomains are geometrically arranged in alternating layers of twins. The findings are consistent with the fundamental underlying assumptions of the ferroelectric adaptive phase theory [Y. M. Jin *et al.*, Phys. Rev. Lett. **91**, 197601 (2003)]. © 2008 American Institute of Physics. [DOI: 10.1063/1.2908228]

Recent structural investigations of $\text{Pb}(\text{Mg}_{1/3}\text{Nb}_{2/3})\text{O}_3\text{-}x\text{PbTiO}_3$ (PMN- x PT) and $\text{Pb}(\text{Zn}_{1/3}\text{Nb}_{2/3})\text{O}_3\text{-}x\text{PbTiO}_3$ (PZN- x PT) single crystals have shown the presence of monoclinic (M) ferroelectric phases in the vicinity of the morphotropic phase boundary (MPB).^{1–6} These M phases are domain engineered states⁷ and serve as structural bridges between the rhombohedral and tetragonal (T) phases that were originally shown in conventional PMN- x PT and PZN- x PT phase diagrams. For PMN- x PT, structural studies by x-ray diffraction and neutron scattering have shown monoclinic M_C , M_A , and M_B phases.^{1–6} The M_C phase belongs to the space group Pm : the unit cell has a unique b_m axis along $[010]$. Both the M_A and M_B phases belong to the Cm space group: the unit cell has a unique b_m axis along $[110]$ and is doubled and rotated 45° about the c axis with respect to the pseudocubic cell: the difference lies in the magnitudes of the components of the polarization. The M_C phase is stable in the vicinity of the MPB for $0.31 < x < 0.37$ (Refs. 1 and 3) in both the zero-field-cooled (ZFC) and (001) field-cooled (FC) conditions; the M_A phase is stable in the ZFC condition for $0.28 < x < 0.31$, and the M_A and M_B phases are stable in the (001) and (110) FC conditions for $0.10 < x < 0.31$,⁵ respectively.

First principles calculations^{8–10} have shown the presence of a polarization rotational instability within these M phases. This approach assumes that the polarization is microscopically homogeneous but requires that the anisotropy barrier of the polarization direction be drastically reduced, which, in turn, implies that the domain wall energy also be dramatically lowered. An alternative adaptive ferroelectric phase theory^{11–13} recently proposed that the M_C phase consists of an inherently structurally heterogeneous state, consisting of conformal miniaturization of stress-accommodating tetragonal twins under the condition of a low domain wall energy. This adaptive state is heterogeneous on the microscale but homogeneous on the macroscale: it cannot be resolved due to limitations of the diffraction optics. In this case, the lattice parameters of the M phase are, in fact, microdomain-averaged ones of the tetragonal phases. In order to achieve

elastic accommodation and avoid lattice misfits along the domain boundaries, particular geometrical invariant conditions between the lattice parameters of the T and M_C phases have been predicted and confirmed. These geometrical restrictions require that the domain-averaged lattice parameters of the M phases follow the twinning relationships of the Wechsler–Lieberman–Read/Bowles–Mackenzie theory^{14,15} of martensitic transformations. Investigations of PMN- x PT have shown that the lattice parameters of the M_C phase are invariant with composition for $0.31 < x < 0.37$, temperature between 100 and 700 K, and applied electric field.^{12,13}

The adaptive ferroelectric phase theory predicts that nanosized tetragonal domains exist within the M_C phase, which are geometrically arranged in alternating layers of twins.^{11–13} The structure of the adaptive phase should have the same morphology as that of the CuAu alloy given in Fig. 1 (Ref. 13) but would be conformally miniaturized to near atomic length scales. However, this has yet to be directly observed by electron microscopy in PMN- x PT or PZN- x PT.

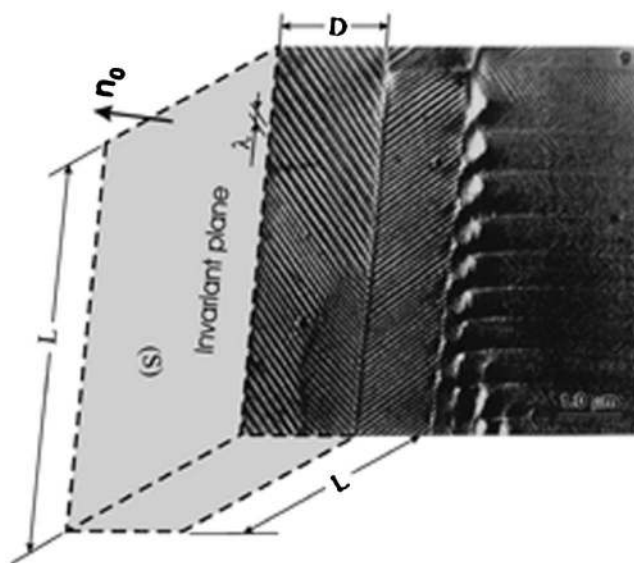


FIG. 1. Dark-field TEM image of a stress-accommodating polydomain structure in a Cu-Au alloy¹⁶ [reproduced with permission from Ref. 13]. The structure of the adaptive phase has the same morphology but is conformally miniaturized to the nanoscale.

^{a)}Electronic mail: somnath.tem@gmail.com.

^{b)}Present address: FEI Company, Eindhoven, The Netherlands.

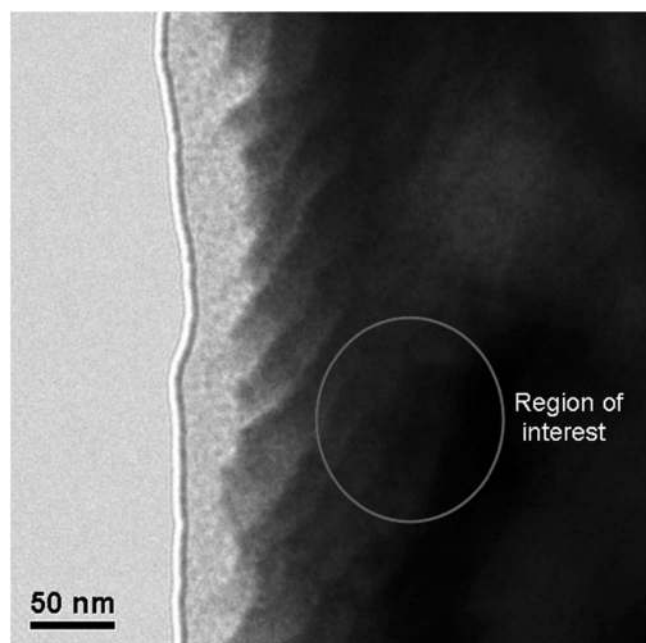


FIG. 2. BF TEM image taken from a [001] PMN-0.35PT single crystal. Note (i) the presence of tweedlike striations as previously reported for MPB compositions of PMN- x PT, and (ii) the red circled region from which HRTEM studies were performed.

In this investigation, we present transmission electron microscopy (TEM) experiments that clearly confirm the presence of such geometrically arranged tetragonal nanotwins within the M_C phase of PMN-0.35PT.

The PMN-0.35PT crystals used in the present study were grown at the Shanghai Institute of Ceramics by using the Bridgman method.^{17,18} Single crystal specimens were cut in a direction perpendicular to [001]. Specimens were prepared by utilizing the standard techniques of grinding, dimpling, and argon-ion-beam thinning (model 1010, Fischione Instrument, PA). Ion-beam thinning has been carried out on both sides of the sample at an inclination angle of 8° of the ion beam with respect to the sample. The bright-field (BF) and high-resolution transmission electron microscopy (HRTEM) experiments were performed by using an FEI TitanTM TEM, which was operated at 200 kV and equipped with a Schottky field emission gun and a postcolumn Gatan image filter. Care was taken to orient the [001] zone axis of the specimen parallel to the incident electron beam before imaging. Images were captured onto a 1024×1024 pixel charge coupled device array. The DIGITAL MICROGRAPH software (Gatan Inc., Pleasanton, CA) was used to analyze the HRTEM lattice images.

Figure 2 shows a BF TEM image that reveals the presence of domainlike striations on the order of several hundred angstrom ($1 \text{ \AA} = 1 \times 10^{-10} \text{ m}$) wide that are oriented along the $\langle 110 \rangle$ direction in the plane of view. Similar domain striations were previously reported in BF images by Xu *et al.*¹⁹ for PMN- x PT for compositions near the MPB and designated as tweedlike structures. In addition, recent investigations by Bai *et al.*²⁰ by using piezoforce microscopy (PFM) revealed a domain hierarchy for (001) oriented PMN-0.35PT. This hierarchy consisted of (i) broad stripelike domains or macro-domain plates oriented close to the $\langle 001 \rangle$ direction with of average size of about $50 \text{ }\mu\text{m}$, as found by polarized light microscopy, within which (ii) alternating domain striations

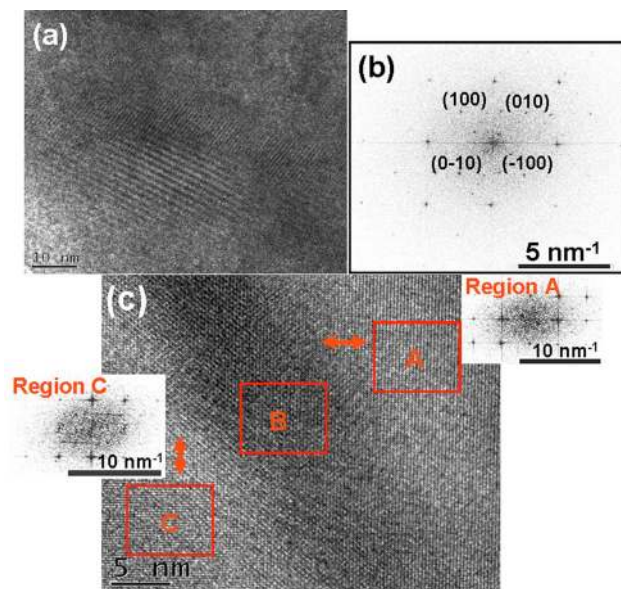


FIG. 3. (Color online) (a) HRTEM image taken from a [001] PMN-0.35PT single crystal; (b) power spectrum (fast Fourier transform) obtained from the image; and (c) HRTEM image taken from a [001] PMN-0.35PT single crystal. Please note the presence of different domain regions in the images designated as A, B, and C; the insets show power spectra (FFT) obtained from (i) region A and (ii) region C.

have been found by using PFM. These striations are oriented close to the $\langle 110 \rangle$ direction, which are similar in morphological features and size to those found in the BF observation in Fig. 2.

Figure 3(a) shows a HRTEM lattice image at a magnification of about $350\,000\times$. In this image, nanometer-sized domains that are geometrically arranged as alternating layers of twins can be seen. The average domain size has been estimated from the contrast to be on the order of $\sim 100 \text{ \AA}$ in width. The length of the domains is $>300 \text{ \AA}$; however, an accurate determination is limited by the field of view in the image at this magnification. A power spectrum, i.e., the square of the magnitude of the complex Fourier transform (intensity distribution), of the image has been obtained, as given in Fig. 3(b). The power spectrum shows four strong $\{100\}$ -type reflections, which are of near equal intensity. These results reveal two structural domain variants oriented along the [100] and [010] directions, and are 90° rotated from each other. It is worth noting that additional reflections of weak intensity in the center portion of the power spectrum [Fig. 3(b)] are caused by the power spectrum calculation and simply originate from the overlap of the two structures.

Figure 3(c) shows another HRTEM lattice image at a higher magnification (around $790\,000\times$). In this image, various nanoregions geometrically arranged as alternating layers are designated as A, B, and C. Two insets, each containing a power spectrum taken from an individual nanoregion, are shown in the figure. In this case, the power spectrum contains two sets of $\{100\}$ -type reflections: one set is stronger in intensity than the other. Comparisons of the spectra taken from regions A and C reveal a 90° rotation between the [100] and [010] orientations of the nanodomains in twin relation.

The images in Figs. 2 and 3 not only reveal the heterogeneous nanotwin nature of PMN-0.35PT but also show some important domain structural features and have close relevance to recent theoretical and computational findings. The TEM image in Fig. 2 shows irregular-shaped domains,

i.e., the domain boundaries are curved instead of straight, as usually expected from crystallographic relationships. This feature is in agreement with a recent thermodynamic analysis,²¹ which showed that the electrocrystalline anisotropy is greatly reduced in the vicinity of the MPB, freeing the polarization direction from preferential polar axes and decoupling polar domains from the crystal lattice. Thus, the domain morphology does not follow the rigorous crystallographic relationships. Moreover, the HRTEM image in Fig. 3(c) indicates a smooth transition region *B* between twin-related nanodomains *A* and *C*, which is a broad domain wall (twin boundary). This observation is in agreement with a recent modeling and simulation,²² which shows that domain wall broadening plays a significant role in nanodomained ferroelectrics. Here, it is worth noting that the nanodomain width and domain wall thickness are of comparable size, which indicates that a significant fraction of the nanodomained ferroelectric materials stays in a transitional domain wall region instead of in the domains. Vanishing electrocrystalline anisotropy and broad domain walls are important issues in MPB-based ferroelectrics and are worthy of further investigation.

Our presented TEM analyses directly reveal the presence of tetragonal nanodomains within the monoclinic M_C phase of PMN-0.35PT, which are geometrically arranged in alternating layers along $\langle 001 \rangle$. These findings confirm the underlying assumption of the adaptive ferroelectric phase theory, wherein the M_C phase of PMN-*x*PT and PZN-*x*PT consists of a structurally heterogeneous state with a high domain wall density that achieves stress accommodation by conformal miniaturization of twinning to near atomic scales.

This work was supported by the Office of Naval Research under N00014-06-1-0204 and MURI N00014-06-1-0530 and by the Department of Energy under DE-FG02-07ER46480.

- ¹B. Noheda, D. E. Cox, G. Shirane, S. E. Park, L. E. Cross, and Z. Zhong, *Phys. Rev. Lett.* **86**, 3891 (2001).
- ²K. Ohwada, K. Hirota, P. W. Rehrig, P. M. Gehring, B. Noheda, Y. Fujii, S. E. E. Park, and G. Shirane, *J. Phys. Soc. Jpn.* **70**, 2778 (2001).
- ³B. Noheda, D. E. Cox, G. Shirane, J. Gao, and Z. G. Ye, *Phys. Rev. B* **66**, 054104 (2002).
- ⁴B. Noheda, Z. Zhong, D. E. Cox, G. Shirane, S. E. Park, and P. Rehrig, *Phys. Rev. B* **65**, 224101 (2002).
- ⁵H. Cao, J. F. Li, D. Viehland, and G. Xu, *Phys. Rev. B* **73**, 184110 (2006).
- ⁶H. Cao, F. Bai, J. F. Li, D. Viehland, G. Xu, H. Hiraka, and G. Shirane, *J. Appl. Phys.* **97**, 094101 (2005).
- ⁷S. E. Park and T. R. Shrout, *J. Appl. Phys.* **82**, 1804 (1997).
- ⁸H. Fu and R. E. Cohen, *Nature (London)* **403**, 281 (2000).
- ⁹A. Garcia and D. Vanderbilt, *Appl. Phys. Lett.* **72**, 2981 (1998).
- ¹⁰L. Bellaiche, A. Garcia, and D. Vanderbilt, *Phys. Rev. Lett.* **84**, 5427 (2000).
- ¹¹D. Viehland, *J. Appl. Phys.* **88**, 4794 (2000).
- ¹²Y. M. Jin, Y. U. Wang, A. G. Khachaturyan, J. F. Li, and D. Viehland, *J. Appl. Phys.* **94**, 3629 (2003).
- ¹³Y. M. Jin, Y. U. Wang, A. G. Khachaturyan, J. F. Li, and D. Viehland, *Phys. Rev. Lett.* **91**, 197601 (2003).
- ¹⁴M. S. Wechsler, D. S. Lieberman, and T. A. Read, *Trans. AIME* **197**, 1053 (1953).
- ¹⁵J. S. Bowles and J. K. Mackenzie, *Acta Metall.* **2**, 129 (1954).
- ¹⁶V. I. Syutkina and E. S. Jakovleva, *Phys. Status Solidi* **21**, 465 (1967).
- ¹⁷W. Tan, Z. Xu, J. Shang, and P. Han, *Appl. Phys. Lett.* **76**, 3732 (2000).
- ¹⁸W. Zhu and P. Han, *Appl. Phys. Lett.* **75**, 3868 (1999).
- ¹⁹Z. Xu, M. Kim, J. F. Li, and D. Viehland, *Philos. Mag. A* **74**, 395 (1996).
- ²⁰F. Bai, J. F. Li, and D. Viehland, *Appl. Phys. Lett.* **85**, 2313 (2004).
- ²¹G. A. Rossetti, Jr., and A. G. Khachaturyan, *Appl. Phys. Lett.* **91**, 072909 (2007).
- ²²W. F. Rao and Y. U. Wang, *Appl. Phys. Lett.* **90**, 041915 (2007).